

Vortex Response and Critical Fields observed via rf penetration depth measurements on the superconductor $\text{YNi}_2\text{B}_2\text{C}$

S. Oxx, D. P. Choudhury, Balam A. Willemssen, H. Srikanth, and S. Sridhar*
*Physics Department, Northeastern University, 360 Huntington Ave.,
Boston, MA 02115*

B. K. Cho and P. C. Canfield
Ames Laboratory, Iowa State University, Ames, IA 50011
(Submitted to Physica C February 19, 1996)

Measurements of the rf penetration depth $\lambda(T, H, \theta)$ are used to study the superconducting order parameter, vortex dynamics in the mixed state and delineate critical fields in the borocarbide superconductor $\text{YNi}_2\text{B}_2\text{C}$. The lower critical field has an anomalous T dependence, $H_{c1}(T) = 1.12 [1 - (T/T_c)]$ kOe, which is however consistent with independent superfluid density measurements at microwave frequencies. The vortex response is dominated by viscous flux flow, indicative of extremely weak pinning, and is parametrized by a field scale $H_{c2, \text{eff}}$. The angular dependence of the vortex contribution $\lambda(\theta)$ is in good agreement with the Coffey-Clem model. Structure is seen in the depairing transition in the vicinity of the upper critical field, with the existence of well-defined critical fields H_{c2a} , H_{c2b} and H_{c2c} , with the vortex field scale $H_{c2, \text{eff}}$ closest to H_{c2b} . Overall the measurements indicate that $\text{YNi}_2\text{B}_2\text{C}$ has a rich and unusual field dependence of its transport parameters.

KEYWORDS: BOROCARBIDE SUPERCONDUCTORS, PENETRATION DEPTH, LOWER CRITICAL FIELD, UPPER CRITICAL FIELD, FLUX PINNING

The borocarbide superconductors $\text{LnNi}_2\text{B}_2\text{C}$ where $\text{Ln} = \{\text{Y, Lu, Tm, Er, Ho and Dy}\}$ [1-3] are a recently discovered family of superconductors with elevated transition temperatures. While there have been numerous studies of these superconductors using traditional probes such as magnetization, specific heat, tunneling, etc. there have been relatively few which directly probe the order parameter and dynamics of vortices

In this paper we report on studies of the radio frequency (rf) penetration depth $\lambda(T, H, \theta)$ of single crystal $\text{YNi}_2\text{B}_2\text{C}$ ($T_c = 15.5$ K) which were carried out in a highly sensitive rf tunnel diode oscillator set-up. The sample is placed in an inductive coil which forms part of a tank circuit, which is self-resonant typically at 3 MHz and is driven by a tunnel diode circuit. Changes in the penetration depth or skin depth of the sample, caused by varying temperature, T , applied dc magnetic field, H , or angle between H and the ab plane, θ , lead to changes in the coil inductance. These are then detected as changes in resonant frequency, and converted to changes in λ via the relation $\delta\lambda(T, H, \theta) \equiv -g [f(T, H, \theta) - f_0(T, H)]$, where g is a geometrical factor set by the sample dimensions and f_0 refers to the resonant frequency without the sample. The very high stability of the circuit, typically 1 Hz in 3 MHz, leads to a very high resolution of the order of a few Å. The technique has been extensively validated through precise measurements in the cuprate superconductors of the non-linear Meissner effect and of vortex parameters such as H_{c1} and pinning force constants [4,5]. In one experimental set-up the sample can be oriented with $H \parallel \hat{c}$ ($\theta = 90^\circ$) or $H \perp \hat{c}$ ($\theta = 0^\circ$), and fields up to 7 T can be applied. In another set-up the

angle θ can be varied continuously between 0° and 90° with an angular accuracy of 0.2° . Here the maximum applied field is 6.4 kOe. In all cases the rf field $H_{\text{rf}} \parallel ab$ and $H_{\text{rf}} \perp H$.

The single crystals of $\text{YNi}_2\text{B}_2\text{C}$ used for these measurements were grown using the Ames Lab Ni_2B flux growth method [6,7]. Crystals grown via this method are in the form of plates with the crystallographic \hat{c} axis perpendicular to the surface of the plate. The crystal used for these measurements has approximate dimensions $1.4 \times 1.2 \times 0.2$ mm³.

I. LOWER CRITICAL FIELD: H_{c1}

Typical results for $\Delta\lambda(T, H, \theta) \equiv \delta\lambda(T, H, \theta) - \delta\lambda(T, H = 0)$ vs. H are shown in Fig. 1, for both $\theta = 0^\circ$ and 90° . The low field portion is further shown in detail in the inset, which reveals essentially no change until a critical field H_{c1} is reached, above which λ increases rapidly. This critical field H_{c1} represents the field at which flux first enters the sample and is governed by both the Meissner state of the superconductor and an effective geometric barrier at the surface. We are justified in calling it the lower critical field as demagnetization corrections are negligible in the case where $H \parallel ab$. Note that the presence of surface barriers would lead to hysteresis in the field dependence of $\Delta\lambda(T, H, \theta)$ at the onset of flux entry. In our data, the observed hysteresis is minimal and is within the experimental resolution. It is also to be noted that surface barrier effects would scale the field values but do not affect the temperature

dependence.

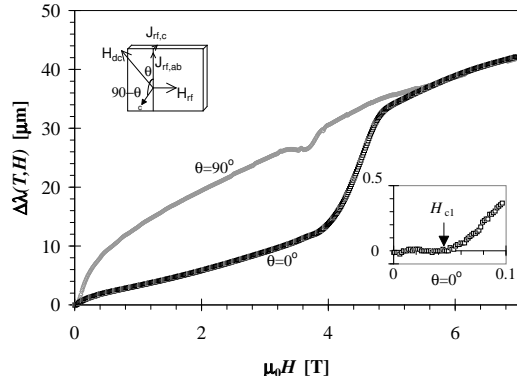


FIG. 1. $\Delta\lambda$ vs. H at $T = 8$ K for $\text{YNi}_2\text{B}_2\text{C}$. (Inset) Expanded plot of low field portion, showing onset at H_{c1} . A schematic of the field/sample orientation is also presented as an inset

Notice that unlike magnetization measurements, where H_{c1} is deduced from deviations from linearity in the $M(H)$ curve, the signature in our data at H_{c1} is very sharp. This is because the experiment effectively measures the flux density $B(H)$ (as will become evident later). Hence, the signature at H_{c1} is a change from zero, and not a change of slope as in $M(H)$ data.

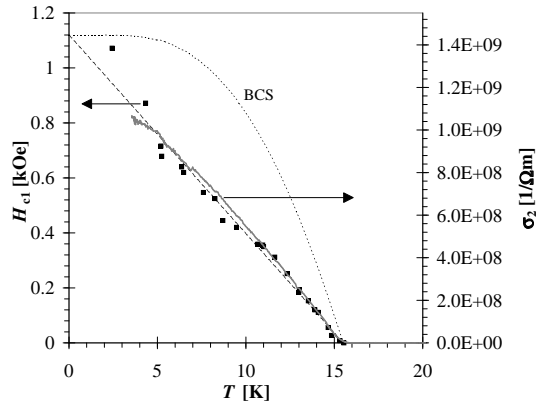


FIG. 2. H_{c1} vs. T . σ_2 vs. T from Ref. [8] is shown for comparison. The dotted line represents a BCS temperature dependence of H_{c1} while the dashed line is a $1-t$ dependence obtained from a least squares fit to the data.

The T dependence of $H_{c1}(T)$ for $\text{YNi}_2\text{B}_2\text{C}$ is shown in Fig. 2. This essentially has a linear behaviour from T_c to 2 K, well represented by $H_{c1}(T) = 1.12(1-t)$ kOe, where $t = T/T_c$. This is unlike that seen in conventional

low T_c superconductors and even differs from the behavior of $\text{YBa}_2\text{Cu}_3\text{O}_{7-\delta}$. However this anomalous behavior finds support in measurements on a related quantity, the superfluid density, measured via the condensate contribution to the complex conductivity, σ_2 , which we have measured elsewhere [8] using a 10 GHz Nb cavity. There, σ_2 was shown to have an anomalous temperature dependence well represented by $\sigma_2(T) = 10^9(1-t)(\Omega\text{m})^{-1}$ (also shown in Fig. 2). Now $\sigma_2 = 1/\mu_0\omega\lambda^2$, and since $H_{c1} \sim (\Phi_0/4\pi\lambda^2)[\ln(\kappa) + 0.5]$, there is a good correlation between the linear temperature dependence of the H_{c1} and σ_2 measurements. (Note that for clean type-II superconductors, κ varies as $1/(1+t^2)$ and thus $\ln(\kappa)$ is expected to have a weak T dependence [9]).

II. VORTEX DYNAMICS AND DEPAIRING

Above H_{c1} , $\lambda(T, H)$ increases strongly in the $\theta = 0^\circ$ case, due to the increasing B in the sample. A similar increase also occurs in the $\theta = 90^\circ$ data, although here the effective $H_{c1} \rightarrow 0$ due to demagnetization. This field dependence $\lambda(H)$ for $H > H_{c1}$ arises from two effects of the magnetic field on the superconductor: depairing of condensed electrons (which dominates when the rf current $J_{rf} \parallel H$) and dynamic vortex response (which dominates when $J_{rf} \perp H$). This is followed by a sharp increase starting and terminating at field values which we call H_{c2a} and H_{c2b} respectively. Above H_{c2b} , λ increases almost linearly with H , which is consistent with the normal state showing a strong positive magnetoresistance. There is an additional field H_{c2c} just above H_{c2b} which can be identified as the point where the $\theta = 0^\circ$ and 90° curves meet as seen in Fig. 1.

We have observed a similarly rich structure in the transition region of the $\text{Ln} = \{\text{Er}, \text{Ho} \text{ and } \text{Dy}\}$ compounds [10]. The presence of multiple structure in the transition region, although interesting in its own right, makes the identification of a single upper critical field H_{c2} somewhat ambiguous. This difficulty is also compounded by the linear- H magnetoresistance in the normal state. All three field scales (H_{c2a} , H_{c2b} and H_{c2c}) agree quantitatively with the H_{c2} values reported in the literature [6]. While the exact origin of this structure is not yet precisely known, its presence in all the borocarbide superconductors we have studied seems to suggest an intrinsic phenomenon and is not likely to be due to spurious chemical phases, as will be presented in a forthcoming publication [10].

In this paper, we focus on the general nature of the depairing and vortex contributions to the rf penetration depth. To test the validity of the standard Coffey-Clem model for the depairing and vortex response in this system, an effective upper critical field H_{c2} coinciding with H_{c2b} is assumed for subsequent analysis. It is to be pointed out that our choice of H_{c2b} as the effective upper

critical field is not arbitrary and is based on other factors like the validity of the Bardeen-Stephen approximation [11] which relates the upper critical field to the flux flow resistivity. A discussion on flux viscosity presented later in the paper will clarify this issue further.

III. DETAILED COMPARISON TO THEORY

We now turn to an understanding of the field dependence of $\lambda(T, H, \theta)$. The principal causes for this field dependence are the depairing effect of $B(H)$ on the condensate and the dynamic response of the vortices to the Lorentz force induced by the rf current. These contributions have been treated self-consistently by Coffey and Clem, leading to the following expression for the complex penetration depth which includes the full angular dependence: [12]

$$\tilde{\lambda} \equiv \lambda - i \frac{R_s}{\mu_0 \omega} = \left[\frac{\lambda_L^2 + \Phi_0 B \sin^2 \theta / \mu_0 (\kappa_p - i \omega \eta)}{1 + i (2 \lambda_L^2 / \delta_{nf}^2)} \right]^{1/2} \quad (1)$$

where $\lambda_L(T, B)$ and $\delta_{nf}(T, B)$ are the condensate penetration depth and the normal-fluid skin depth in the superconducting state, and $\kappa_p(T)$ and $\eta(T)$ are the vortex pinning force constant and viscosity respectively. The field-dependence of the condensate background is represented by $\lambda_L^2(T, B) = \lambda_{L0}^2 f(T, B)$ and $\delta_{nf}^2(T, B) = \delta_n^2(T, B) [1 - f(T, B)]$, where for instance $f(T, B) = [1 - (T/T_c)^4] [1 - (B/B_{c2})]$ in a two-fluid model. For $\theta = 0^\circ$, the rf currents in the ab plane are parallel to the vortices and hence the Lorentz force is zero for those vortices at the sample faces. (A schematic representation of the relative orientations of H_{rf} and the rf current, J_{rf} , with respect to H is shown as an inset in Fig. 1). Thus the vortex response is mostly absent in the $\theta = 0^\circ$ case, except for a small contribution of order $O(d/W) \sim 0.1$ from the edges, where d and W are the sample thickness and width respectively. This can be incorporated phenomenologically in terms of an aspect ratio $r \equiv [1 + (d/W)^{-1}]^{-1}$ which mixes the vortex contribution ($\theta = 90^\circ$) to the force-free ($\theta = 0^\circ$) term as $\sqrt{\tilde{\lambda}_{||}^2 + r \tilde{\lambda}_{\perp}^2}$. The angular dependence provides a nice way of separating out the depairing and the vortex contributions to the penetration depth.

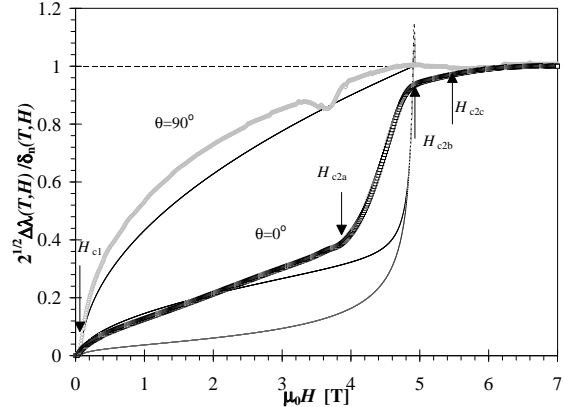


FIG. 3. $2^{1/2} \Delta \lambda(T, H) / \delta_n(T, H)$ vs. H at $T = 8$ K and $\theta = 0^\circ$ and 90° . The solid lines represent theoretical calculations based on Eq. 1 for the two orientations presented, including finite aspect ratio effects for the $\theta = 0^\circ$ case with $r = 0.11$. The dotted line ignores the effects of finite aspect ratio. The dashed horizontal line represents the normal state skin depth.

In Fig. 3 we present the same data as in Fig. 1 normalized with respect to $\delta_n(T, H) / \sqrt{2}$. Motivated by the observation that the field dependence of $\delta_n(T < T_c, H > H_{c2})$ follows that of $\delta_n(T > T_c, H)$ we have used $\delta_n(T, H) \approx \delta_n(T > T_c, H)$ for this normalization. Theoretical calculations based on Eq. 1, taking into account the small aspect ratio as discussed earlier and also assuming negligible pinning (i.e. $\kappa_p \rightarrow 0$), are shown in Fig. 3 along with the data. For the vortex contribution, at fixed frequency f the response is pinning dominated if $f < f_c$ and viscosity dominated if $f > f_c$, where $f_c = \kappa_p / 2\pi\eta$. It is quite striking that pinning is negligible even at 3 MHz, which would effectively imply that flux is in free flow as soon as vortices enter the sample above H_{c1} . This is in contrast to the estimated f_c values of 20 GHz in $\text{YBa}_2\text{Cu}_3\text{O}_{7-\delta}$ [13] and ~ 100 MHz in low T_c materials [14]. For $\theta = 0^\circ$, the low field variation of λ is adequately reproduced by the calculation, confirming the presence of a finite vortex contribution consistent with the aspect ratio independently determined from the sample dimensions.

The $\theta = 90^\circ$ data shows a dip at a field below the effective H_{c2} . This can result from sudden changes in pinning or scattering which are parametrized by the terms κ_p and η in Eq. 1. A rise in κ_p at a threshold field can be associated with the “peak effect” commonly seen in type-II superconductors with weak pinning. The signature of the peak effect is a peak in critical current density and would show up as a dip in the rf susceptibility, which is what we are effectively measuring in the $\theta = 90^\circ$ case. There is a general consensus that the peak effect arises due to enhanced pinning as a result of a rapidly decreasing rigidity

of the vortex lattice just below H_{c2} [15]. However, there is still some controversy over whether it is a softening of the tilt modulus (C_{44}) or shear modulus (C_{66}) that leads to this decrease in rigidity [16–18]. An alternate possibility is that this dip feature is due to an anomalous field dependence of η arising as a result of unusual quasiparticle scattering in the superconducting state. Since the effect is much stronger in the vortex response rather than the depairing, this is an indication that the scattering due to bound quasiparticle states in the normal vortex cores could also be responsible for the observed dip in the $\theta = 90^\circ$ data below the effective H_{c2} .

When the vortex term dominates as at $\theta = 90^\circ$, the $\lambda(T, H)$ data can be used to extract the pinning forces and viscosity as we have done elsewhere in both single crystals and films of $\text{YBa}_2\text{Cu}_3\text{O}_{7-\delta}$ [5,13]. A Bardeen-Stephen estimate of the viscosity can be made using $\eta_{\text{BS}}(T, B) = \Phi_0 B_{c2}(T)/\rho_n(T, B)$, which yields $\eta_{\text{BS}}(0, 0) \sim 1 \times 10^{-6}$ Ns/m² for $\text{YNi}_2\text{B}_2\text{C}$, compared to values of $\sim 10^{-8}$ Ns/m² for Nb.

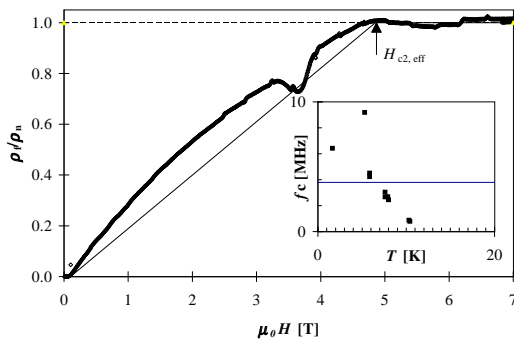


FIG. 4. Flux flow resistivity ρ_f/ρ_n obtained from the $\theta = 90^\circ$ data in Fig. 3. The solid line indicates the expected Bardeen-Stephen behavior. The dashed horizontal line indicates the normal state resistivity. (inset) $f_c = \kappa_p/\eta$ vs. T extracted from the relative peak height is presented as an inset. The horizontal line in the inset indicates the measurement frequency.

The data in Fig. 3 can also be presented as the normalized flux flow resistivity $\rho_f/\rho_n \equiv 2\lambda^2(T, B)/\delta_n^2(T, B)$ which is presented as a function of H for $T/T_c = 0.5$ in Fig. 4. The flux flow resistivity approaches the normal state almost linearly with a slope $1/B_{c2, \text{eff}}$ ($\sim 1/B_{c2}$) consistent with the observations of Gittleman and Rosenblum in conventional superconductors [14]. Overall the response appears to be well described by Eq. 1 assuming $\eta = \eta_{\text{BS}}(T, B)$ and $\kappa_p \rightarrow 0$, consistent with magnetization experiments which have also shown evidence for extremely weak pinning [19]. The differences between

the observed response and theoretical Bardeen-Stephen response (indicated by the solid line in Fig. 4) can be attributed to an underestimate of $\rho_n(T, B)$ in the superconducting state as well as some variation of $\kappa_p(T)$. If the dip observed in the $\theta = 90^\circ$ data is associated with a change in pinning, we can estimate the change in κ_p in the peak region from the relative depth of the dip since $\eta_{\text{eff}} \sim \eta/(1 + \kappa_p/\omega\eta)$. A plot of $f_{c, \text{peak}} = \kappa_p/2\pi\eta(T)$ extracted in this form is shown in the inset to Fig. 4.

IV. ANGULAR DEPENDENCE

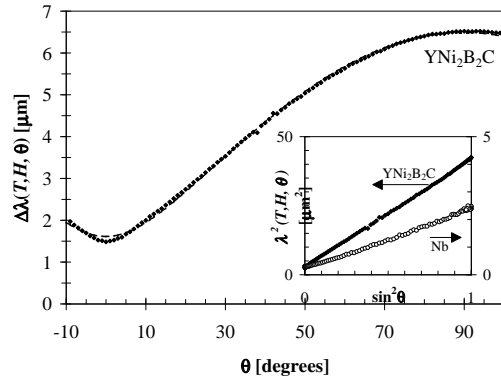


FIG. 5. $\Delta\lambda$ vs. θ at $T = 8$ K and $H = 1$ kOe. The line represents a least squares fit to Eq. 1. (Inset) λ^2 vs. $\sin^2 \theta$ for the same data for comparison with Eq. 1. A plot for polycrystalline Nb at $T = 7$ K and $H = 1.5$ kOe is also shown.

The full angular dependence of λ for $H_{c1} < H < H_{c2a}$ is shown in Fig. 5 along with the fit generated using Eq. 1. The inset shows λ^2 plotted against $\sin^2 \theta$ for the same data. A similar plot for a poly-crystalline Nb sample of comparable dimensions is also shown in the panel. The excellent agreement between the experimental data and the Coffey-Clem expression of Eq. 1 is obvious from the good fit and also the linear dependence of λ^2 with $\sin^2 \theta$. The slopes are vastly different for $\text{YNi}_2\text{B}_2\text{C}$ and Nb as the response is pinning dominated in Nb whereas pinning is almost irrelevant in $\text{YNi}_2\text{B}_2\text{C}$ at 3 MHz. The Coffey-Clem calculation as presented in Eq. 1 assumes an isotropic H_{c2} case and from the good fit with the $\text{YNi}_2\text{B}_2\text{C}$ data one can infer that the effective H_{c2} is generally isotropic in this system [6], although a slight deviation of the data from the model at low angles might indicate the presence of some degree of anisotropy in these layered systems. Elsewhere we have observed unusual angular dependence and anisotropy effects in $\text{HoNi}_2\text{B}_2\text{C}$ related to magnetic order and details about this will be given in a separate publication.

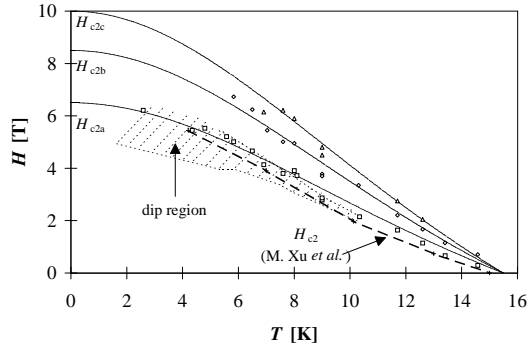


FIG. 6. H_{c2a} , H_{c2b} and H_{c2c} vs. T obtained from the $\theta = 0^\circ$ data. Lines representing a $(1 - t^2)/(1 + t^2)$ dependence are overlaid. H_{c2} values from Ref. [6] are indicated by the thick dashed line. The region where the dip is observed in the $\theta = 90^\circ$ data is indicated by the dotted hatch lines.

The magnitude and T dependence of the three features in the vicinity of H_{c2} for $\text{YNi}_2\text{B}_2\text{C}$ (H_{c2a} , H_{c2b} and H_{c2c}) are shown in Fig. 6 are in good agreement with those determined by magnetization measurements [6] and the overall temperature dependence is fit reasonably well by a $(1 - t^2)/(1 + t^2)$ form. Two aspects make the observed onset field H_{c2a} extremely interesting: H_{c2a} is located at about the same field where the dip is seen in the ($\theta = 90^\circ$) data and occurs further from the effective upper critical field than would otherwise be expected. The theoretical calculation fails to reproduce the finite slope of the transition, which would imply an unusual field dependence of $\lambda(B)$. Looking at it in a different way, the simple variation of the superfluid density ($= \lambda_0^2/\lambda^2$) as $(1 - B/B_{c2})$ within the framework of a two-fluid model breaks down and one has to assume a stronger reduction in the superfluid density as $B \rightarrow B_{c2}$. Note that earlier studies on $\text{YNi}_2\text{B}_2\text{C}$ [8] using a superconducting Nb cavity at 10 GHz also indicated disagreement with BCS or two-fluid models in the T dependence of the surface resistance and penetration depth, as displayed in Fig. 2 in terms of $\sigma_2(T)$. This may indicate the existence of scattering of unknown origin in the superconducting state. We believe the origin of H_{c2a} could result from this anomalous scattering or vortex lattice softening/melting or a combination of both these effects. Whatever the cause, the underlying dependence of $\Delta\lambda(T, H, \theta = 0)$ in the vicinity of H_{c2a} is masked to some extent by the mixing of vortex and depairing terms in the ($\theta = 0^\circ$) data.

In conclusion, the rf measurements presented here reveal a rich variety of electrodynamic response in the superconducting state of the non-magnetic borocarbide superconductor $\text{YNi}_2\text{B}_2\text{C}$. In particular, $\lambda(T, H = 0)$ and H_{c1} both have anomalous non BCS T dependences. The

experiments have very high sensitivity which enable observation of subtle effects on the superconducting order parameter and the vortex lattice due to the applied field. A unique way of studying the vortex response and field-induced depairing individually by variation of θ is presented. The angular dependence of $\lambda(T, H, \theta)$ is well described by the Coffey-Clem theory with an isotropic H_{c2} . A dip is observed in the vortex response which can be related to a change in pinning (and thus to the “peak effect”) or alternatively to anomalous scattering in the mixed state. Pinning is found to be extremely weak, and consequently, the crossover frequency is expected to be orders of magnitude lower than that of most conventional and high- T_c superconductors. Structure is observed in the depairing transition from the superconducting to normal state, which is also found to have an anomalous H dependence. Thus although $\text{YNi}_2\text{B}_2\text{C}$ is in many ways a conventional high- κ type-II superconductor, the high frequency measurements appear to indicate many unconventional properties of the Meissner and mixed states.

Work at Northeastern was supported by grant NSF-DMR-9223850. Ames Laboratory is operated for the U. S. Department of Energy by Iowa State University under Contract No. W-7405-Eng-82. Work at Ames was supported by the Director for Energy Research, Office of Basic Energy Sciences.

* E-mail: srinivas@neu.edu

- [1] R. Nagarajan, C. Mazumdar, Z. Hossain, S. K. Dhar, K. V. Gopalakrishnan, L. C. Gupta, C. Godart, B. D. Padalia, and R. Vijayaraghavan, Phys. Rev. Lett. **72**, 274 (1994).
- [2] R. J. Cava, H. Takagi, B. Battlog, H. W. Zandbergen, J. J. Krajewski, W. F. P. jr., R. B. van Dover, R. F. Felder, T. Siegrist, K. Mizuhaski, J. O. Lee, H. Eisaki, S. A. Carter, and S. Uchida, Nature **367**, 146 (1994).
- [3] B. K. Cho, P. C. Canfield, L. L. Miller, and D. C. Johnston, Phys. Rev. B **52**, R3844 (1995).
- [4] S. Sridhar, D.-H. Wu, and W. L. Kennedy, Phys. Rev. Lett. **63**, 1873 (1989).
- [5] D.-H. Wu and S. Sridhar, Phys. Rev. Lett. **65**, 2074 (1990).
- [6] M. Xu, P. C. Canfield, J. E. Ostenson, D. K. Finnemore, B. K. Cho, Z. R. Want, D. C. Johnston, and D. E. Farrell, Physica C **227**, 321 (1994).
- [7] B. K. Cho, M. Xu, P. C. Canfield, L. L. Miller, and D. C. Johnston, Phys. Rev. B **52**, 3676 (1995).
- [8] T. Jacobs, B. A. Willemsen, S. Sridhar, P. C. Canifield, and B. K. Cho, Phys. Rev. B **52**, R7022 (1995).
- [9] R. D. Parks, editor, *Superconductivity*, Marcel Dekker, Inc., New York, 1969.
- [10] S. Sridhar et al., in preparation.
- [11] J. Bardeen and M. J. Stephen, Phys. Rev. **140**, A1197

- (1965).
- [12] M. W. Coffey and J. R. Clem, Phys. Rev. B **45**, 9872 (1992).
- [13] B. A. Willemsen, J. S. Derov, J. H. Silva, and S. Sridhar, Appl. Phys. Lett. **67**, 551 (1995).
- [14] J. I. Gittleman and B. Rosenblum, Proc. IEEE , 1138 (1964).
- [15] A. I. Larkin and Y. N. Ovchinnikov, J. Low. Temp. Phys. **34**, 409 (1979).
- [16] E. H. Brandt, J. Low. Temp. Phys. **26**, 709 (1977).
- [17] E. H. Brandt, Phys. Rev. B **34**, 6514 (1986).
- [18] X. Ling, C. Tang, S. Bhattacharya, and P. M. Chaikin, Peak effect in superconductors: Melting of larkin domains, from cond-mat. 9504109
- [19] M. Xu and P. C. Canfield, private communication.